PHYSICAL REVIEW MATERIALS **1**, 040401(R) (2017)

Kinetically limited composition of ternary III-V nanowires

Jonas Johansson[1,*] and Masoomeh Ghasemi[1,2]
[1]*Solid State Physics and NanoLund, Lund University, Box 118, 221 00 Lund, Sweden*
[2]*Division of Computational Thermodynamics, KTH Royal Institute of Technology, Stockholm, Sweden*
(Received 21 June 2017; revised manuscript received 29 August 2017; published 28 September 2017)

Controlling the composition of ternary III-V semiconductor nanowires is of high technological importance and the current theoretical understanding is so far limited. We derive a model for the kinetically limited composition of metal-particle-seeded, ternary nanowires. The model is based on the diffusion controlled growth rate of supercritical nuclei. Applying this model to gold-seeded and self-seeded growth of $In_xGa_{1-x}As$ we are able to explain the experimentally observed features related to nanowire compositions, including the attainability of compositions within the miscibility gap. By directly comparing with experiments we find that 2% arsenic in the alloy particle during self-seeded growth of InGaAs nanowires is a realistic assumption.

DOI: 10.1103/PhysRevMaterials.1.040401

Band-gap engineering is an important enabling technology for electronic and optoelectronic applications of III-V semiconductor nanowires. The most straightforward approach to band-gap engineering in nanowires is composition control in ternary nanowires, both for radial and longitudinal growth. There are a few experimental investigations with the aim to control the composition in ternary nanowires, and perhaps the most investigated system is InGaAs [1–7]. Other experimentally investigated ternary nanowire systems are InGaSb [8], AlGaAs [9–12], InAsSb [13,14], and GaAsSb [15,16]. Even if Dubrovskii [17] has proposed a model, relating the composition of the solid nanowire to the composition of the vapor phase during growth, the theoretical understanding of how the composition of the particle influences the composition of the nanowire is still limited. To bridge this gap, the aim of the current investigation is to explain how the nanowire composition during longitudinal, particle-seeded growth depends on the composition of the seed alloy particle.

We have previously discussed the composition of ternary III-V nanowires in the nucleation limited regime, approximating the composition of the solid material with the composition of the critical nucleus [18]. In the current investigation we follow up on our previous work and propose a model for the kinetically limited composition of metal-particle-seeded ternary III-V nanowires. The model is based on diffusion controlled growth of supercritical nuclei within two-component nucleation theory. We derive the model for the general case and then we discuss it in terms of gold-seeded and self-seeded $In_xGa_{1-x}As$ nanowire growth. In this case, the diffusion of As is rate limiting, and we find that the composition of the nanowire is independent on diffusion and depends only on chemical potential differences.

As a model system, consider the growth of $A_xB_{1-x}D$ nanowires from a liquid metal particle with A, B, and D dissolved in the seed metal U. The growth rate of the nucleus is given by the respective differences in attachment and detachment rates, and since the detachment rates are difficult to estimate they are usually eliminated using detailed balance [19]. This results in the following expression for the growth rates of the two species AD and BD [20],

$$\frac{di}{dt} = W_i\left(1 - e^{\frac{\partial F}{\partial i}}\right), \tag{1}$$

where i is the number of AD pairs in the growing nucleus, W_i is the attachment rate of AD pairs, and F is the formation energy of the (i, j) nucleus in units of RT (the gas constant and the temperature in degrees Kelvin). The growth rate of BD is described by a similar expression in j instead of i. The formation energy can be written as [18]

$$F = -i\Delta\mu_i - j\Delta\mu_j + a\sqrt{i+j}, \tag{2}$$

where the $\Delta\mu$'s are chemical potential differences between the species in the liquid phase (L) and the solid phase (S) [21] and a is proportional to the surface energy of the cluster. The chemical potential differences are given by

$$\Delta\mu_i = \mu_A^L + \mu_D^L - \mu_{AD}^0 - RT\ln x - \omega(1-x)^2, \tag{3a}$$

$$\Delta\mu_j = \mu_B^L + \mu_D^L - \mu_{BD}^0 - RT\ln(1-x) - \omega x^2, \tag{3b}$$

where μ_{AD}^0 and μ_{BD}^0 are the chemical potentials for pure AD and BD, respectively, x is the composition of the solid, and ω is the interaction parameter describing the interaction between AD and BD. For sufficiently large clusters, the surface energy term in Eq. (2) is negligible and the partial derivatives in Eq. (1) can be approximated as $\partial F/\partial i = -\Delta\mu_i$ and $\partial F/\partial j = -\Delta\mu_j$, since $i\partial\Delta\mu_i/\partial i + j\partial\Delta\mu_j/\partial i = i\partial\Delta\mu_i/\partial j + j\partial\Delta\mu_j/\partial j = 0$.

For large enough chemical potential differences, the detachment rates are negligible and the clusters grow irreversibly governed by purely kinetic effects, which in the VLS (vapor-liquid-solid) case discussed here means diffusion controlled growth [20,22],

$$\frac{di}{dt} = ChJ_i, \tag{4}$$

where C is the circumference and h is the thickness of a cluster. The parameter J_i is the effective flux of AD pairs into the (i, j) cluster. The A, B, and D atoms are dissolved in the liquid metal and thus diffuse separately. However, both atoms in the AD and BD pairs are simultaneously needed to form the crystal, and the minority component will limit the incorporation rate. Therefore we model the effective fluxes of AD and BD into the

*Corresponding author: jonas.johansson@ftf.lth.se

growing cluster as

$$\frac{1}{J_i} = \frac{1}{J_A} + \frac{1}{J_D}, \tag{5}$$

and similarly for J_j. The diffusive fluxes are expressed by Fick's first law,

$$J_I = \frac{D_I}{\Omega_I}\frac{dc_I}{dz}, \tag{6}$$

where D_I is the diffusivity and Ω_I is the atomic volume of species I ($I = A$, B, and D) in the liquid metal particle and the other factor is the concentration gradient (in atomic fraction) of I at the perimeter of the cluster. In most cases a linear diffusion profile is a good approximation, and we can write

$$J_I = \frac{D_I}{\Omega_I}\frac{c_I - c_I^{\mathrm{eq}}}{\delta_I}, \tag{7}$$

where c_I is the concentration of I away from the cluster and c_I^{eq} is the concentration of the liquid in equilibrium with the solid cluster. The length δ_I describes the distance over which the concentration outside the cluster changes. Here, there are two interesting limiting cases: the *diffusion regime* where δ_I is much larger than the nucleus (but still limited by the size of the metal particle), and the *ballistic regime* (or attachment limited regime) where δ_I is much smaller than the nucleus [20]. Dubrovskii and Grecenkov [22] considered the ballistic regime with $\delta = \sqrt{\Omega_S/h}$ in their recent description of nucleation in VLS growth. Combining Eqs. (1), (4), and (5) we identify the attachment rates W_i and W_j as

$$W_i = Ch\frac{J_A J_D}{J_A + J_D}, \tag{8a}$$

$$W_j = Ch\frac{J_B J_D}{J_B + J_D}. \tag{8b}$$

At sufficiently long growth times, the thermodynamically defined composition of the critical nucleus corresponding to a saddle point in F is forgotten, and instead the composition of the growing nucleus is dictated by kinetics [23]. To derive an expression for this composition, we differentiate the composition $x = i/(i + j)$ with respect to time t. By setting $dx/dt = 0$, we arrive at the stationary kinetic composition of the solid phase,

$$x_k = \frac{di/dt}{di/dt + dj/dt}, \tag{9}$$

which, using Eqs. (1) and (8) can be rewritten as

$$\frac{1}{x_k} = 1 + \frac{J_B(J_A + J_D)}{J_A(J_B + J_D)}\frac{1 - e^{-\Delta\mu_j}}{1 - e^{-\Delta\mu_i}}, \tag{10}$$

where the equilibrium concentrations [see Eq. (7)] as well as the chemical potentials all are evaluated at x_k. Equation (10) is our first central result and is in agreement with Stauffer's result [23].

Unless further approximations are made, there is no closed form solution to Eq. (10) and it has to be solved numerically. However, since x_k is a solution to an autonomous nonlinear differential equation, the stability of x_k is not guaranteed but must be checked for all solutions. Stability is, however, ensured if $f'(x_k) < 0$, where the prime denotes differentiation with respect to x, and $f(x) = W_i(1 - e^{-\Delta\mu_i}) - x[W_i(1 - e^{-\Delta\mu_i}) + W_j(1 - e^{-\Delta\mu_j})]$. We remind the reader that W_i, W_j, and the chemical potential differences are all functions of x. There is a possibility that Eq. (10) has more than one solution and the stability of each of these solutions must be tested. Only a stable solution where both $\Delta\mu_i$ and $\Delta\mu_j$ are positive can result in a stable steady state composition of a two-component, growing nucleus.

In the following, we apply our model to predict the kinetically limited composition of gold alloy particle-seeded $In_xGa_{1-x}As$ nanowires grown with the VLS mechanism. Since the diffusivity of As has been estimated to be 3–4 orders of magnitude smaller than the diffusivities of In and Ga [22,24,25], and since the concentration differences in Eq. (7) are about one order of magnitude smaller for As than for In and Ga, it is safe to assume that the growth is As limited. In this case, the stationary kinetic composition is independent on diffusivities and given by

$$\frac{1}{x_k} = 1 + \frac{1 - e^{-\Delta\mu_j}}{1 - e^{-\Delta\mu_i}}. \tag{11}$$

This expression is thus valid both in the diffusion and in the ballistic regimes. We note that both $\Delta\mu_i$ and $\Delta\mu_j$ are composition dependent and evaluated at $x = x_k$. Since we use the regular solution model, the interaction between the $i =$ InAs and $j =$ GaAs pairs is considered, so that In and Ga effectively compete for the group III sublattice sites of the growing nucleus.

As discussed above for the general case, stability is ensured if $\Delta\mu_i > 0$, $\Delta\mu_j > 0$, and

$$e^{-\Delta\mu_i}[1 + (1 - x)\Delta\mu_i'] + e^{-\Delta\mu_j}[1 - x\Delta\mu_j'] - 2 < 0, \tag{12}$$

at $x = x_k$, where the chemical potential derivatives are given by

$$\Delta\mu_i' = -RT\frac{1}{x} + 2\omega(1 - x), \tag{13a}$$

$$\Delta\mu_j' = RT\frac{1}{1 - x} - 2\omega x. \tag{13b}$$

For the derivation of Eq. (12) we have used that J_{As} is almost independent on x. This, together with our analytic expression for the chemical potential differences, give us the tools to calculate x_k for gold alloy particle-seeded $In_xGa_{1-x}As$ nanowires. In particular, we will investigate the difference between gold-seeded and self-seeded (or gold-free) growth. We shall assume that the wires are wide enough, so that stationary compositions can be reached. That is, the wire radius is always larger than the size of the critical nucleus.

In Fig. 1 we show the kinetic steady state composition x_k as a function of the In fraction y of the total amount of group III in the liquid particle ($y = c_{\mathrm{In}}/c_3$ with $c_3 = c_{\mathrm{In}} + c_{\mathrm{Ga}}$). The curves were calculated for $T = 750$ K, $c_{\mathrm{As}} = 0.02$, and for varying group III concentrations, $c_3 = 0.3$ (blue), $c_3 = 0.5$ (black), $c_3 = 0.7$ (red), and $c_3 = 0.98$ (green). At these conditions it is clear that all compositions of the solid phase can be reached, even if it seems very difficult to reproducibly control the composition beyond $x_k = 0.5$, since this requires

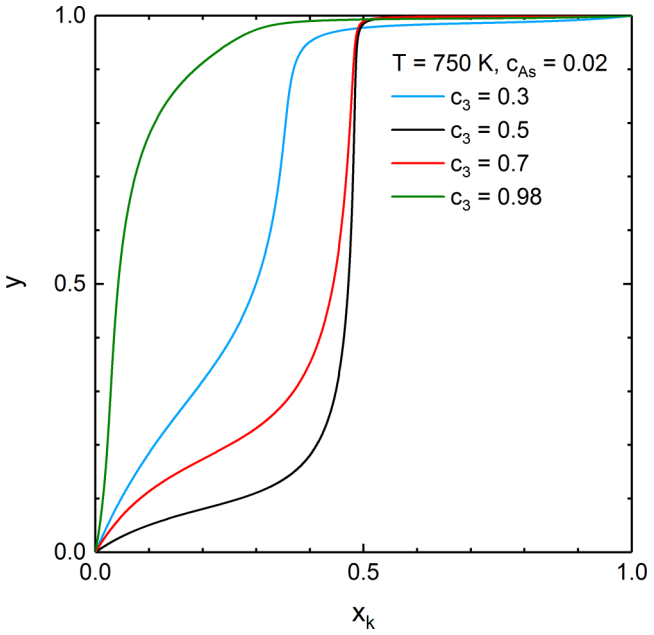

FIG. 1. The steady state InAs composition of the supercritical nucleus x_k as a function of the In fraction of the group III content y at $T = 750$ K and an As molar fraction of $c_{\mathrm{As}} = 0.02$. The total group III molar fraction was varied from $c_3 = 0.3$ to 0.98.

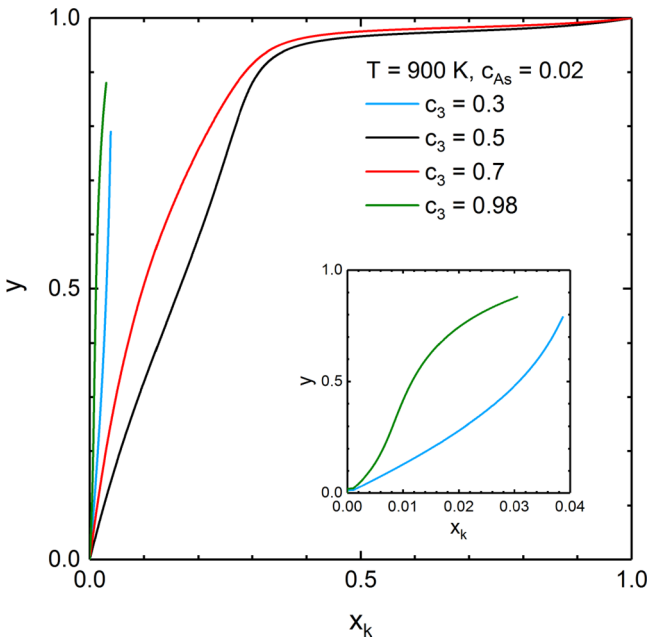

FIG. 2. Same as in Fig. 1 but the composition curves account for $T = 900$ K. The inset shows a zoomed view of the $c_3 = 0.3$ and 0.98 curves.

y values very close to one. This is especially the case for $c_3 = 0.5$ and 0.7. According to our previous investigation [18] these cases represent the highest supersaturation, that is, $\Delta\mu_i$ and $\Delta\mu_j$ are larger for $c_3 = 0.5$ and 0.7 than for $c_3 = 0.3$ and 0.98, and that is the reason that these curves tend to $x_k = 0.5$ for sufficiently high $y < 1$. For larger y values, approaching 1, $\Delta\mu_j$ decreases so that x_k finally reaches 1.

According to Eq. (11), x_k approaches 0.5 for large $\Delta\mu_i$ and $\Delta\mu_j$, which is consistent with the purely kinetic composition considered by Fisenko and Wilemski [26], $x_k = W_i/(W_i + W_j)$. In our case, $W_i = W_j$, since the diffusion of As limits both InAs and GaAs incorporation, which gives $x_k = 0.5$ in the purely kinetic regime. For $c_3 = 0.5$, both chemical potentials are sufficiently large over a range of y values to give compositions of the solid nanowire close to $x_k = 0.5$.

In Fig. 2, we show the kinetic steady state composition x_k as a function of the In fraction y of the total amount of group III in the liquid particle for the same conditions as in Fig. 1, with the exception that the temperature is $T = 900$ K, that is, 150 K higher. At these conditions, the supersaturation is much lower due to increased solubilities. It is intriguing that the $c_3 = 0.3$ and 0.98 curves could not be calculated for all values of y but end at specific values of y, approximately 0.8 and 0.9, respectively. The reason for this is that for sufficiently high y, one or both of the chemical potentials become negative. This corresponds to undersaturation in one or both components leading to the dissolution of the nucleus and potentially unstable growth or no growth at all. In these cases, the maximum achievable concentration of the solid is $x_k = 0.03-0.04$. The prospect of composition control is more promising for the $c_3 = 0.5$ and 0.7 cases. These curves are not attracted to $x_k = 0.5$ and they have steeper slopes for y close to 1 than the corresponding curves for $T = 750$ K. The case $c_3 = 0.5$ should be particularly interesting for composition control. The curve is approximately linearly increasing with one slope up to $y \approx 0.90$ and another, smaller slope from $y \approx 0.95$ to 1. Due to the small chemical potentials, the $c_3 = 0.5$ and 0.7 curves can be approximated by $x_k \approx \Delta\mu_i$ for $0 < y \lesssim 0.5$ and $x_k \approx 1 - \Delta\mu_j$ for $0.95 \lesssim y < 1$.

Next, we compare our findings to previous experimental investigations. Wu *et al.* [5] have grown gold catalyzed InGaAs nanowires using metal-organic vapor phase epitaxy at $T = 703-743$ K. By changing the composition in the vapor phase, they were able to control the composition in the nanowire. The nanowire top composition differed from the bottom composition in a way that the bottom parts were InAs enriched. These nanowires were tapered and the bottom InAs enrichment was attributed to radial growth, whereas the top part growth was attributed to gold-particle-seeded growth, which is the case to which our model applies. From the postgrowth compositional analysis data obtained by Wu *et al.* [5] we estimate that the seed particles contain about 70% gold and that the amount of gallium is negligible, as is the amount of arsenic, which is expected due to its low solubility in gold and group III melts. The top, VLS grown part of these nanowires contain about 50% InAs, and this agrees with the $c_3 = 0.3$ curve with y close to one. We note that 50% InAs could also be achieved during growth at higher supersaturation. If, for instance, the particles during growth ($T = 723$ K) had a $c_3 = 0.35$ and a $c_{\mathrm{As}} = 0.05$, the composition control curve would be qualitatively similar to the $c_3 = 0.5$ curve in Fig. 1 so that 50% InAs in the nanowires ($x_k = 0.5$) would be easy to achieve for a range of y values. We do not believe that this is the case, however, since nanowire composition can be controlled from $x_k \approx 0.15$ up to $x_k \approx 0.80$ [5], which indicates a lower slope of the $x_k - y$ curve than what can be achieved in the high supersaturation case. One should also note that both c_3 and c_{As}

could vary with y in such a way that composition control would be easier (lower slopes of the $x_k - y$ curves). Here, it is particularly interesting to note that also thermodynamically unstable compositions can be reached. At temperatures below 816 K, there is a miscibility gap in the solid $In_xGa_{1-x}As$ solution and because of this, compositions around $x = 0.5$ are not thermodynamically stable (at temperatures lower than this). However, our model explains that these compositions are readily attainable during growth at high supersaturation irrespective of temperature.

Heiss *et al.* [1] report on self-catalyzed, gold-free growth of $In_xGa_{1-x}As$ nanowires. In order to suppress sidewall and substrate incorporation of InAs they use a low As beam flux and a high temperature, $T = 903$ K. They report a maximum amount of 4%–5% InAs in the nanowires. Indeed, this is in great agreement with the $c_3 = 0.98$ curve in Fig. 2. At these conditions, y can be increased up to 0.88, corresponding to $x_k = 0.03$ (see inset in Fig. 2). When $y > 0.88$, the liquid gets undersaturated and growth ceases. Decreasing the temperature and increasing the As beam flux would in theory lead to higher supersaturation, but in practice this leads to sidewall and substrate growth. Increasing the In flux leads to less reproducible growth [1]. From our calculations we find that for self-seeded growth at 900 K, the more As in the seed particle, the higher can y be before the supersaturation is lost. In order to have a supersaturated seed particle at all values of y at these conditions, a very high As concentration of $c_{As} > 0.08$ is required.

In a later investigation by Heiss *et al.* [27] it was concluded that if self-seeded $In_xGa_{1-x}As$ nanowires could be grown at lower temperatures, it should be possible to increase their InAs content. What led to this conclusion was the observation that the top parts of the nanowires, close to the seed particle, were InAs enriched and that was attributed to increased InAs incorporation during the cooling down phase after growth. More specifically, the highest In concentration in the seed particle was 80% and the top 40 nm of the nanowire had an InAs concentration of 40% [27]. Using our model we readily predict that self-seeded growth with $c_{As} = 0.02$ and $y = 0.80$ gives $x_k = 0.4$ at the temperature $T = 663$ K (which is a temperature high enough for growth).

Finally, returning to gold alloy particle-seeded growth, Jung *et al.* [3] report that they can completely tune the composition of $In_xGa_{1-x}As$ nanowires over the entire interval, $0 < x < 1$. They use a relatively simple growth method based on thermal evaporation of InAs and GaAs powders and the composition of the nanowires depend on the InAs-GaAs powder ratio. Their growth temperature is quite high, $T = 1073$ K. According to our calculations, in order to have stable growth for all y values at $c_3 = 0.5$, resulting in composition control over the entire range of x_k values, a very high c_{As} of about 0.15 is needed.

In conclusion, we have calculated the kinetically limited composition of gold-alloy-seeded and self-seeded $In_xGa_{1-x}As$ nanowires. Judging from our calculations we predict that self-seeded growth with composition control should be carried out at low temperature. This is in part supported by experiments, but composition controlled growth at low temperature remains technically challenging due to InAs sidewall growth. On the other hand, composition controlled, gold-alloy-seeded growth should be carried out at high temperature, where the $x_k - y$ curves seem more favorable for composition control over the entire range of x_k values. The arsenic concentration in the particle during growth is unknown, but our comparisons with the experiments by Heiss *et al.* [1] indicate that 2% is a realistic assumption for self-seeded growth at around 900 K. Finally, we note that our model for kinetically limited growth explains the experimental observations of compositions within the miscibility gap.

We gratefully acknowledge financial support from NanoLund (the Center for Nanoscience at Lund University), the Swedish Research Council (VR), and the Knut and Alice Wallenberg Foundation (KAW).

[1] M. Heiss, A. Gustafsson, S. Conesa-Boj, F. Peiro, J. R. Morante, G. Abstreiter, J. Arbiol, L. Samuelson, and A. F. I. Morral, Catalyst-free nanowires with axial $In_xGa_{1-x}As$/GaAs heterostructures, Nanotechnology **20**, 075603 (2009).

[2] F. Jabeen, V. Grillo, F. Martelli, and S. Rubini, InGaAs/GaAs core-shell nanowires grown by molecular beam epitaxy, IEEE J. Sel. Top. Quantum Electron. **17**, 794 (2011).

[3] C. S. Jung, H. S. Kim, G. B. Jung, K. J. Gong, Y. J. Cho, S. Y. Jang, C. H. Kim, C. W. Lee, and J. Park, Composition and phase tuned InGaAs alloy nanowires, J. Phys. Chem. C **115**, 7843 (2011).

[4] Y. N. Guo, T. Burgess, Q. Gao, H. H. Tan, C. Jagadish, and J. Zou, Polarity-driven nonuniform composition in InGaAs nanowires, Nano Lett. **13**, 5085 (2013).

[5] J. Wu, B. M. Borg, D. Jacobsson, K. A. Dick, and L. E. Wernersson, Control of composition and morphology in InGaAs nanowires grown by metalorganic vapor phase epitaxy, J. Cryst. Growth **383**, 158 (2013).

[6] A. S. Ameruddin, P. Caroff, H. H. Tan, C. Jagadish, and V. G. Dubrovskii, Understanding the growth and composition evolution of gold-seeded ternary InGaAs nanowires, Nanoscale **7**, 16266 (2015).

[7] A. S. Ameruddin, H. A. Fonseka, P. Caroff, J. Wong-Leung, R. L. M. O. H. Veld, J. L. Boland, M. B. Johnston, H. H. Tan, and C. Jagadish, $In_xGa_{1-x}As$ nanowires with uniform composition, pure wurtzite crystal phase and taper-free morphology, Nanotechnology **26**, 205604 (2015).

[8] S. G. Ghalamestani, M. Ek, B. Ganjipour, C. Thelander, J. Johansson, P. Caroff, and K. A. Dick, Demonstration of defect-free and composition tunable $Ga_xIn_{1-x}Sb$ nanowires, Nano Lett. **12**, 4914 (2012).

[9] Z. H. Wu, M. Sun, X. Y. Mei, and H. E. Ruda, Growth and photoluminescence characteristics of AlGaAs nanowires, Appl. Phys. Lett. **85**, 657 (2004).

[10] C. Chen, N. Braidy, C. Couteau, C. Fradin, G. Weihs, and R. LaPierre, Multiple quantum well AlGaAs nanowires, Nano Lett. **8**, 495 (2008).

[11] J. W. Guo, H. Huang, Y. Z. Ding, Z. Y. Ji, M. Liu, X. M. Ren, X. Zhang, and Y. Q. Huang, Growth of zinc blende GaAs/AlGaAs heterostructure nanowires on Si substrate

by using AlGaAs buffer layers, J. Cryst. Growth **359**, 30 (2012).

[12] G. Priante, F. Glas, G. Patriarche, K. Pantzas, F. Oehler, and J. C. Harmand, Sharpening the interfaces of axial heterostructures in self-catalyzed AIGaAs nanowires: Experiment and theory, Nano Lett. **16**, 1917 (2016).

[13] B. M. Borg, K. A. Dick, J. Eymery, and L.-E. Wernersson, Enhanced Sb incorporation in InAsSb nanowires grown by metalorganic vapor phase epitaxy, Appl. Phys. Lett. **98**, 113104 (2011).

[14] L. Namazi, S. G. Ghalamestani, S. Lehmann, R. R. Zamani, and K. A. Dick, Direct nucleation, morphology and compositional tuning of $InAs_{1-x}Sb_x$ nanowires on InAs (111) B substrates, Nanotechnology **28**, 165601 (2017).

[15] E. Ahmad, S. K. Ojha, P. K. Kasanaboina, C. L. Reynolds, Y. Liu, and S. Iyer, Bandgap tuning in $GaAs_{1-x}Sb_x$ axial nanowires grown by Ga-assisted molecular beam epitaxy, Semicond. Sci. Technol. **32**, 035002 (2017).

[16] L. X. Li, D. Pan, Y. Z. Xue, X. L. Wang, M. L. Lin, D. Su, Q. L. Zhang, X. Z. Yu, H. So, D. H. Wei, B. Q. Sun, P. H. Tan, A. L. Pan, and J. H. Zhao, Near full-composition-range high-quality $GaAs_{1-x}Sb_x$ nanowires grown by molecular-beam epitaxy, Nano Lett. **17**, 622 (2017).

[17] V. G. Dubrovskii, Fully analytical description for the composition of ternary vapor-liquid solid nanowires, Cryst. Growth Des. **15**, 5738 (2015).

[18] J. Johansson and M. Ghasemi, Composition of gold alloy seeded InGaAs nanowires in the nucleation limited regime, Cryst. Growth Des. **17**, 1630 (2017).

[19] D. Kashchiev, *Nucleation: Basic Theory with Applications* (Butterworth Heinemann, Oxford, UK, 2000).

[20] V. G. Dubrovskii, *Nucleation: Theory and Growth of Nanostructures* (Springer, Berlin, 2014).

[21] J. Grecenkov, V. G. Dubrovskii, M. Ghasemi, and J. Johansson, Quaternary chemical potentials for gold-catalyzed growth of ternary InGaAs nanowires, Cryst. Growth Des. **16**, 4526 (2016).

[22] V. G. Dubrovskii and J. Grecenkov, Zeldovich nucleation rate, self-consistency renormalization, and crystal phase of Au-catalyzed GaAs nanowires, Cryst. Growth Des. **15**, 340 (2015).

[23] D. Stauffer, Kinetic theory of two-component ("heteromolecular") nucleation and condensation, J. Aerosol Sci. **7**, 319 (1976).

[24] Y. Andre, K. Lekhal, P. Hoggan, G. Avit, F. Cadiz, A. Rowe, D. Paget, E. Petit, C. Leroux, A. Trassoudaine, M. R. Ramdani, G. Monier, D. Colas, R. Ajib, D. Castelluci, and E. Gil, Vapor liquid solid-hydride vapor phase epitaxy (VLS-HVPE) growth of ultra-long defect-free GaAs nanowires: *Ab initio* simulations supporting center nucleation, J. Chem. Phys. **140**, 194706 (2014).

[25] A. K. Roy and R. P. Chhabra, Prediction of solute diffusion coefficients in liquid metals, Metall. Trans. A **19**, 273 (1988).

[26] S. P. Fisenko and G. Wilemski, Kinetics of binary nucleation of vapors in size and composition space, Phys. Rev. E **70**, 056119 (2004).

[27] M. Heiss, B. Ketterer, E. Uccelli, J. R. Morante, J. Arbiol, and A. F. I. Morral, In(Ga)As quantum dot formation on group-III assisted catalyst-free InGaAs nanowires, Nanotechnol. **22**, 195601 (2011).